# HOMOGENEOUS NUCLEATION OF DISLOCATIONS

*A. Carpio*[1], *I. Plans*[2], *L.L. Bonilla*[2]

[1] Departamento de Matemática Aplicada, Universidad Complutense de Madrid, 28040 Madrid, Spain

[2] G. Millán Institute of Modeling, Simulation and Industrial Mathematics, Universidad Carlos III de Madrid, 28911 Leganés, Spain

ana_carpio@mat.ucm.es, ignacio.plans@uc3m.es, bonilla@ing.uc3m.es

**ABSTRACT:** When a two-dimensional crystal described by a dissipative discrete elasticity model is sheared beyond a critical stress $F = F_c$, the strained dislocation-free state becomes unstable via a subcritical pitchfork bifurcation. Numerical continuation shows that configurations containing two or four edge dislocations become simultaneously stable in appropriate stress ranges. Selecting a fixed final applied stress $F_f > F_c$, these stable configurations may be reached by setting $F = F_f t/t_r$ during different time intervals $t_r$. At a characteristic time after $t_r$, one or two dipoles are nucleated, split, and the resulting two edge dislocations move in opposite directions to the sample boundary.

**Keywords:** Discrete dislocation models, homogeneous nucleation of edge dislocations, subcritical bifurcation, numerical continuation

## 1 INTRODUCTION

Homogeneous nucleation of dislocations is observed in different processes such as nanoindentation experiments [1], heteroepitaxial crystal growth [2] and indentation experiments in colloidal crystals [3] or soap bubble raft models [4]. Homogeneous nucleation of dislocations occurs in a perfect crystal and is therefore expected to have a much higher activation energy than heterogeneous nucleation at defect sites such as step edges. Different types of calculations have been used to interpret homogeneous nucleation of dislocations in different situations, ranging from atomistic simulations to continuum mechanics interpretations or combinations thereof [5]. In all cases, a reliable nucleation criterion is needed to capture the nature of nucleated defects and the time and place at which such defects appear.

In this paper, we tackle homogeneous nucleation of dislocations as a bifurcation problem in discrete elasticity. Discrete elasticity models of dislocations in cubic crystals [6, 7] describe dislocation cores in a natural way, their equations are asymptotic to the correct anisotropic elasticity far from defect cores and have been used to analyze dislocation depinning and motion at the Peierls stress in a precise manner [8]. Here we consider a simple 2D discrete elasticity model that may describe homogeneous nucleation of edge dislocations and is amenable to detailed analysis. Stationary solutions whose displacement profile exhibits dislocations bifurcate subcritically from a dislocation free static solution at a critical value of an applied shear stress. Ramping the stress from zero to values larger than the critical stress, we can select different stable stationary configurations containing dislocations that proceed from homogeneously nucleated dislocation dipoles that later split and move in opposite directions.

## 2 MODEL AND BIFURCATION PHENOMENA

We consider a 2D simple cubic lattice with lattice constant normalized to 1, lattice points labelled by indexes $(i, j)$, $i = 1, ..., N_x$ and $j = 1, ..., N_y$, and displacement

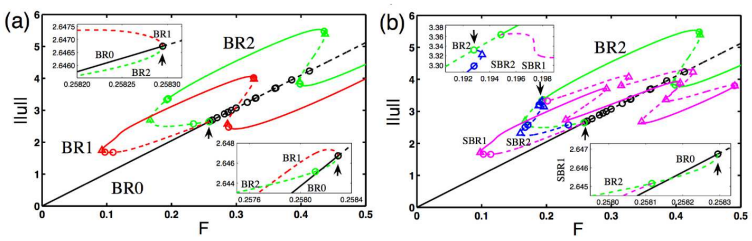


Figure 1: (a) Bifurcation diagram showing only the primary stationary branches issuing from the homogeneous solution BR0. At $F_c$, branches BR1 and BR2 appear as a subcritical pitchfork bifurcation from BR0 (see the insets). (b) Bifurcation diagram in which BR1 has been omitted and secondary bifurcation branches SBR1 and SBR2 issuing from BR2 are shown. Zooms near the bifurcation points are shown in the insets. In all cases, solid lines correspond to stable solutions, dashed lines to unstable solutions, limit points are marked as triangles and bifurcation points as circles. Parameter values are: $A = 1$, $a = 0.25$.

vector $(u_{i,j}, 0, 0)$. At the boundary, a shear strain $F$ is applied, so that the displacement $u_{i,j}$ for $j = 1, N_y$ and for $i = 1, N_x$ is $F\,[j - (N_y + 1)/2]$. $F$ is also the dimensionless shear stress. The components of the displacement vector in the $y$ and $z$ directions are ignored. $u_{i,j}$ obeys the following nondimensional equations:

$$\mu \frac{\partial^2 u_{i,j}}{\partial t^2} + \alpha \frac{\partial u_{i,j}}{\partial t} = u_{i+1,j} - 2u_{i,j} + u_{i-1,j} + A\,[g_a(u_{i,j+1} - u_{i,j}) + g_a(u_{i,j-1} - u_{i,j})]. \quad (1)$$

Here $A = C_{44}/C_{11}$ for cubic crystals with elastic constants $C_{11}$, $C_{12}$, $C_{44}$. Selecting a nondimensional time scale $C_{11}t/(\rho\gamma l^2) \to t$, we have $\alpha = 1$, $\mu = C_{11}/(\rho l^2 \gamma^2)$, where $\gamma$, $\rho$ and $l$ are a friction coefficient with units of frequency, the mass density and the dimensional lattice constant, respectively. The nondimensional displacement vector is measured in units of $l$. The overdamped case corresponds to $\mu = 0$. On the other hand, selecting a nondimensional time scale $C_{11}^{1/2}t/(l\rho^{1/2}) \to t$, we have $\mu = 1$, $\alpha = l\gamma\sqrt{\rho/C_{11}}$. Then the conservative case corresponds to $\alpha = 0$. The nonlinear function $g_a$ is periodic, with period equal to the space lattice and $g_a'(0) = 1$. In our simulations, we have used

$$g_a(x) = \begin{cases} \frac{2a}{\pi} \sin\left(\frac{\pi x}{2a}\right), & \text{if } -a \le x \le a, \\ \frac{2a}{\pi} \sin\left(\frac{\pi}{2} \frac{x-1/2}{a-1/2}\right), & \text{if } a \le x \le 1-a, \end{cases} \quad (2)$$

with $0 \le a \le 1/2$ and period 1. In the symmetric case $a = 1/4$, (2) is the interacting atomic chains model [11], which is a simplification of the discrete elasticity models in Ref. [6]. The parameter $a$ controls the asymmetry of $g_a$, which in turn determines the size of the dislocation core and the Peierls stress $F_c$ needed for a dislocation to start moving [8]. As $a$ increases, so does the Peierls stress, whereas both the core size and the mobility of defects decrease. Large values of $a$ result in very narrow cores and large Peierls stresses. We have observed that $F_c$ is slightly larger than $a$ and that $F_c$ approaches $a$ as the lattice size increases. For $a = 0.25$, $F_c$ is 0.258 for a 6x6 lattice and 0.252 for a 12x12 lattice.

We consider the overdamped case, $\mu = 0$, $\alpha = 1$ with $A = 1$, $a = 0.25$. In the unstressed crystal configuration $F = 0$, a given initial condition evolves exponentially fast to a stable homogeneous dislocation-free stationary state BR0. As we select larger

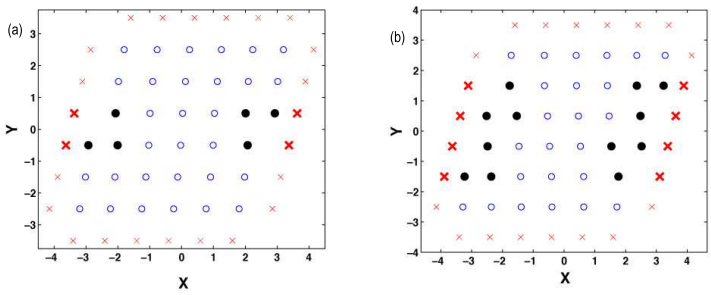


Figure 2: Configurations of the stationary solutions (a) BR1, (b) BR2, at $F_f = 0.259$. The crosses represents the positions of the boundary atoms which are fixed by the shear boundary condition.

and larger positive stresses, the homogeneous stationary configuration is strained but continues to be stable and dislocation-free until a critical stress $F_c$ is reached. At $F_c$ a subcritical pitchfork bifurcation occurs, as the global bifurcation diagram in Fig. 1(a) shows. The complete bifurcation diagram of the $l^2$ norm of the displacement vector versus $F$ has been calculated using the AUTO program of numerical continuation of solutions [12]. This diagram is rather complex with many bifurcation points issuing from different stationary solution branches, most of which are unstable. If we depict all possible solution branches, the resulting bifurcation diagram is rather messy. Thus we have chosen to depict only important solution branches which are stable in certain stress intervals. In Fig. 1 we observe that only two primary branches bifurcate from BR0 at $F = F_c = 0.2193$. Both start being unstable for $F$ close to $F_c$ but become stable after limit points (BR1 exactly after the limit point, BR2 becomes stable after a secondary bifurcation point with $F > F_{l2}$), giving rise to intervals were several stationary solutions are simultaneously stable and, as we will see later, can be reached according to the stress history. In its stable part, BR1 is a stationary configuration containing two edge dislocations with opposite Burgers vectors which have their origin in the nucleation of a dislocation dipole which is later split. In its stable part, BR2 contains four edge dislocations originating from nucleation and splitting of two dipoles. See Fig. 2. For other stress values, the configurations corresponding to BR1 and BR2 are similar to those shown in this figure. We have not depicted many small secondary and tertiary branches joining different bifurcation points in the diagram, for otherwise it would become cluttered and unusable. These branches are mostly unstable or, if they are stable, their basins of attraction are very small. While BR1 and BR2 persist in samples of different size, the location of secondary bifurcation and limit points and the configurations for secondary solution branches depend on the size and shape of the crystal. There are secondary branches SBR1 and SBR2 bifurcating from BR2 that are stable in certain stress ranges as shown in Fig. 1(b). Actually, each of these lines represent two solution branches having the same $l^2$ norm. In their stable ranges, the configurations of SBR1 and SBR2 exhibit two and four edge dislocations originating from splitting of one and two dipoles, respectively. The configurations of SBR1 mimic those of BR1, but their two edge dislocations are not centered: they are shifted upwards (for one of the solution branches having the same norm) and downwards (for the other solution branch). A reflection from the horizontal axis crossing the lattice center transforms one configuration in the other. In the case of SBR2, there are only two narrow ranges of $F$ in which the stationary solutions are stable. The range closer to the upper part of branch BR2 is similar to that described before for SBR1, but now there are four edge dislocations instead of two. The other range with smaller values of $F$ produces configurations that are more curious: while two edge dislocations have moved to the boundaries in opposite directions, the other two dislocations form either

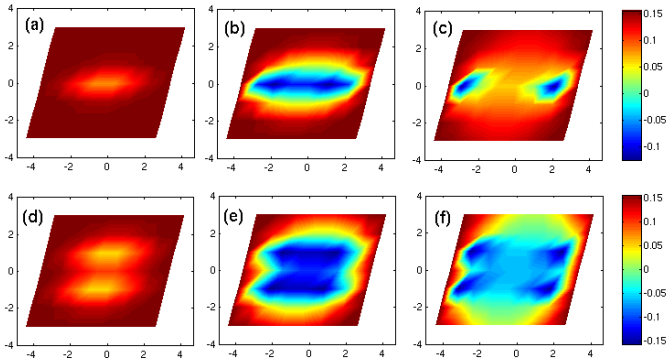


Figure 3: Upper panel from left to right: Snapshots of the strain $2e_{12}$ at times (a) 280.8, (b) 282.9, (c) 377.8 for the evolution towards BR1 with ramping time $t_r = 85$ ($c = 3.047 \times 10^{-3}$). Lower panel from left to right: Same at times (d) 302.4, (e) 304.7, (f) 393.0 for the evolution towards BR2 with ramping time $t_r = 100$ ($c = 2.59 \times 10^{-3}$). $F_f = 0.259$.

a dipole or a dislocation loop *inside the lattice*, depending on which of the two solutions with the same $l^2$ norm is considered. It turns out that the strain fields of these two solutions have opposite signs at each lattice point. We have not depicted many small secondary and tertiary unstable branches joining different bifurcation points in the diagram, for otherwise it would become cluttered and unusable.

We have found ranges of $F$ at which two or more stationary solutions are simultaneously stable. Thus we would expect to evolve to one or another of these solutions depending on the way we stress the sample. One way to proceed is to start from the stable stationary configuration BR0 at $F = 0$. We then increase $F$ to a small value $\Delta F$, use the configuration BR0 for $F = 0$ as initial condition, solve (1) and find the corresponding stable stationary configuration. Repeating this procedure, we follow BR0 until $F_c$ and for $F > F_c$ we obtain the configuration BR2 at the corresponding value of $F$. Can we obtain other configurations doing things differently? The answer is yes. Suppose that we want to explore the stable stationary configurations at a stress $F_f = 0.259$ slightly larger than $F_c = 0.25829$. Starting with BR0 at $F = 0$, we turn in the stress according to a linear law: $F(t) = ct\,H(t_r - t) + F_f H(t - t_r)$, where $c = F_f/t_r$, $t_r$ is the ramping time and $H(x)$ is the Heaviside unit step function. Same as in other multistable systems [13], the final configuration is either BR2 or BR1 depending on the final stress and the ramping time. At the time dislocations are nucleated, the displacement vector departs significantly from BR0.

Fig. 3 shows several snapshots of the strain component $2e_{12} = g_a(u_{i,j+1} - u_{i,j})$ taken after the stress has reached its final value $F_f$ and $u_{i,j}$ is evolving towards its final stationary configuration. In the upper panel of Fig. 3, we observe a depression of the strain $e_{12}$ at the sample center that indicates nucleation of a dislocation dipole. At later times, this dipole is split in two edge dislocations of opposite Burgers vector that move towards the boundaries in opposite directions. The final configuration is BR1. Similarly, for longer ramping times, two dislocation dipoles are nucleated, each splits into two edge dislocations with opposite Burgers vectors that then move towards the boundaries in opposite directions. The final result is BR2. It is interesting to observe that, at the time dipoles are nucleated, the strain components for the respective snapshots are very close to those of the unstable parts of the stationary solution branches BR1 and BR2. If we follow the unstable branch of BR1 backwards from the limit point for $F_{l1} \approx 0.11$ to the critical stress $F_c$, we observe that its strain

$2e_{12}$ has a depression at the center of the sample corresponding to dipole nucleation for $F_{l1} < F < F_c$, but this depression becomes less and less observable as we approach $F_c$. Similarly, the unstable part of $BR2$ from its limit point $F_{l2} \approx 0.17$ to $F_c$ first exhibits two symmetric depressions near the center of the sample corresponding to nucleation of two dipoles. Then these depressions diminish until the configuration of the unstable part of BR2 becomes very similar to that of BR1 as $F$ approaches $F_c$. This is as it should be for BR1 and BR2 merge at $F_c$ in a subcritical pitchfork bifurcation. Near $F_c$, BR1 and BR2 differ from BR0 by $\pm\beta\psi_{i,j}$. Here $\beta \propto \sqrt{F_c - F}$ and $\psi_{i,j}$ is the eigenvector corresponding to the largest eigenvalue of the linearized problem about BR0, $\lambda_0(F_c) = 0$.

We have presented numerical solutions corresponding to a 6x6 lattice. We have observed that the value of $F_c$ and the shape of the bifurcation diagram do not change qualitatively if we increase the computational domain, for example to a 12x12 lattice. The primary branch BR1 acquires more limit points but its configuration in the stress range where BR1 is stable still corresponds to nucleation of one dipole which is split into two edge dislocations later, each moving to the boundaries in opposite directions as $F$ varies. The branch BR2 appears now superimposed to BR1 in the bifurcation diagram because the corresponding configurations are symmetric with respect to the horizontal axis and therefore have the same $l^2$ norm. The reflection symmetry with respect to the horizontal axis in the middle of the crystal is typical for lattices with an odd number of atoms $N_x$, $N_y$. Therefore each branch in the bifurcation diagram using the $l^2$ norm of the displacement vector corresponds to two different solution branches with the same norm and symmetric configurations. The bifurcation diagrams of rectangular lattices are similar to those of square ones, but we have observed a few differences: sometimes the pitchfork bifurcation at $F_c$ is supercritical, but both bifurcating branches have a limit point for a slightly higher stress and become unstable, repeating then the pattern of the square lattice diagrams.

Now what are the effects of inertia? The bifurcation diagram corresponding to stationary solutions is still the same as presented here. However, the stability character of the solutions changes. In the conservative case $m = 1$, $\alpha = 0$, stable solutions are no longer asymptotically stable. Linearizing (1) about a stable solution, we find a problem with purely imaginary eigenvalues. Therefore these solutions are centers: small disturbances about them give rise to small permanent oscillations about them. The linearized problem about unstable solutions has pairs of positive and negative eigenvalues and therefore these solutions are saddle-centers in general.

What have we learned about an instability and dislocation nucleation criterion from our bifurcation study? Clearly $F_c$ marks the instability of the homogeneous solution branch BR0 and dislocations are nucleated at stress values more or less close to $F_c$, although the fact that the bifurcation is subcritical makes it important to determine the stresses at which the solution branches BR1 and BR2 become stable. This cannot be done by simple linear stability calculations: instead numerical continuation algorithms such as AUTO have to be employed. $F_c$ is characterized as the stress value at which the largest eigenvalue of the linear eigenvalue problem about BR0 becomes zero. As it is well-known, we can determine the largest eigenvalue by solving the minimization problem of a quadratic functional $\sum_{ijkl} \varphi_{i,j} \mathcal{L}_{i,j,k,l} \varphi_{k,l}$ over the class of square summable vectors $\varphi_{i,j}$. The relation of this problem to the $\Lambda$ criterion [5] remains unclear. In the present case of a perfect lattice under shear, the critical resolved shear stress criterion used to interpret nanoindentation experiments [1] does not seem relevant. Related results can be found in [9]. Similar models for a simplified 2D nano indentation setting [10] characterize the jumps observed in nanoindentation strain/stress curves in terms of a related class of bifurcations, and given a mathematical basis to their connection with dislocation loop nucleation.

## 3 CONCLUSIONS

We have analyzed 2D samples of a material described by a simple discrete elasticity model. Under shear stress, the homogeneous dislocation-free stationary solution becomes lineally unstable at a critical stress $F_c$. At this stress two stationary branches bifurcate subcritically from it forming a pitchfork bifurcation. Consider overdamped dynamics first. One of these branches (far from the bifurcation point) becomes stable and its configuration corresponds to nucleation of a dislocation dipole, splitting thereof and motion of the resulting edge dislocations with opposite Burgers vectors to opposite sites in the sample boundary. The other branch eventually becomes stable too and its configuration corresponds to nucleation and splitting of two dislocation dipoles, that give rise to four edge dislocations. To obtain different stable branches that coexist at the same value of a supercritical stress, ramping the stress over a time period of variable duration is used. Slow ramping leads to the final configuration with four dislocations, whereas appropriately fast ramping leads to the stationary configuration with only two edge dislocations. This bifurcation picture seems to describe larger lattices and it describes the stationary solutions even if inertia is added.


### Acknowledgments

Work financed by the MEC grants MAT2005-05730-C02-01 (LLB & IP), MAT2005-05730-C02-02 (AC) and BES-2003-1610 (IP). We thank Dr. J. Galán for help with AUTO.


### References


[1] A. Asenjo, M. Jaafar, E. Carrasco and J.M. Rojo. Dislocation mechanisms in the first stage of plasticity of nanoindented Au(111) surfaces. *Phys. Rev. B* 73:075431, 2006.

[2] K.R. Breen, P.N. Uppal and J.S. Ahearn. Homogeneous nucleation of dislocations in $In_{0.4}Ga_{0.6}As$/GaAs near critical thickness. *J. Vac. Sci. Technol. B* 8:730–735, 1990.

[3] P. Schall, I. Cohen, D. Weitz and F. Spaepen. Visualizing dislocation nucleation by indenting colloidal crystals. *Nature* 440:319–323, 2006.

[4] A. Gouldstone, K.J. Van Vliet and S. Suresh. Simulation of defect nucleation in a crystal. *Nature* 411:656, 2001.

[5] J. Li, K.J. Van Vliet, T. Zhu, S. Yip and S. Suresh. Atomistic mechanisms governing elastic limit and incipient plasticity in crystals. *Nature* 418:307–310, 2002.

[6] A. Carpio and L. L. Bonilla. Discrete models of dislocations and their motion in cubic crystals. *Phys. Rev. B* 71:134105, 2005.

[7] L.L. Bonilla, A. Carpio and I. Plans. Dislocations in cubic crystals described by discrete models. *Physica A* 376:361–377, 2007.

[8] A. Carpio and L.L. Bonilla. Edge dislocations in crystal structures considered as traveling waves of discrete models. *Phys. Rev. Lett.* 90:135502, 2003.

[9] A. Carpio, I. Plans, L.L. Bonilla. Homogeneous nucleation of dislocations in a periodized discrete elasticity model. *EPL (Europhysics Letters)* 81:36001, 2008.

[10] A. Carpio, I. Plans and L.L. Bonilla. Toy nanoindentation model and incipient plasticity. *Chaos, solitons and fractals* 42:1623–1630, 2009.

[11] A. I. Landau, A.S. Kovalev and A. D. Kondratyuk. Model of interacting atomic chains and its application to the description of the crowdion in an anisotropic crystal. *Phys. stat. sol. (b)* 179:373–381, 1993.

[12] E.J. Doedel, R.C. Paffenroth, A.R. Champneys, T.F. Fairgrieve, Yu.A. Kuznetsov, B.E. Oldeman, B. Sandstede and X. Wang. AUTO2000: Continuation and bifurcation software for ordinary differential equations (with HomCont). Technical Report, Concordia University, 2002. `https://sourceforge.net/projects/auto2000/`

[13] L.L. Bonilla, R. Escobedo and G. Dell'Acqua. Voltage switching and domain relocation in semiconductor superlattices. *Phys. Rev. B* 73:115341, 2006.